Chemical Engineering Journal 161 (2010) 114–121

Contents lists available at ScienceDirect

Chemical Engineering Journal

journal homepage: www.elsevier.com/locate/cej

The application of iron coated activated alumina, ferric oxihydroxide and granular activated carbon in removing humic substances from water and wastewater: Column studies

Majeda Khraisheh[a,*], Mohammad A. Al-Ghouti[b], Cecile Andrea Stanford[c]

[a] Department of Chemical Engineering, Qatar University, P.O. Box 2713, Doha, Qatar
[b] Industrial Chemistry Centre, Royal Scientific Society (RSS), P.O. Box: 143, Amman, Jordan
[c] Southern Water, Southern House, Lewes Road, Falmer, Brighton BN1 9PY, UK

ARTICLE INFO

Article history:
Received 20 August 2009
Received in revised form 4 April 2010
Accepted 23 April 2010

Keywords:
Adsorption
Humic substances
Water treatment
Activated carbon
Column studies activated alumina

ABSTRACT

The efficiency of iron coated activated alumina, ferric oxihydroxide and granular activated carbon for the removal of humic substance (HS) from water and wastewater was demonstrated in batch studies. This paper investigated the use of these successful adsorption–adsorbate systems in a continuous flow mode in an effort to obtain the required design and operational data; essential for successful application in water treatment works. The adsorbents were used individually. The influence of the various molecular mass fractions on the adsorption ability of the various systems was considered. Fractionation of humic substances was carried out and low, medium and high molecular mass fractions were produced. Two different column diameters (2.5 and 1 cm) were used in the experimental runs. The smaller diameter column was used for experiments dealing with the lower molecular weigh humics as these are very difficult to produce in large enough quantities to carry out continuous adsorption runs in the traditional 2.5 cm diameter laboratory adsorption columns. The dissolved organic content (DOC), ultraviolet (UV) absorbance and specific ultraviolet absorbance (SUVA) values were measure and analysed under different operating conditions. Furthermore, the experimental results were modelled using the Thomas model and the empty bed contact time model (EBCT). The Mass Transfer Zone was also analysed for all cases. The results indicated strongly the influence of molecular mass in the adsorption of humic substances. In addition, two distinctive features appear from these results; GAC is able to remove high MM although lacking of mesoporosity (attributed to precipitation and alteration of HS conformation) and β-FeOOH does not show such a high adsorption capacity as previously predicted, attributed to the non-equilibrium state and to the lack of surface under the media compaction.

1. Introduction

Humic substances represent a wide range of non-biodegradable organic matter that needs to be removed from drinking water supply. In rivers, lakes and ground waters; which are to the basis of this work: humics come from the leaching of soils, sediments, aquatic animal and vegetal life, as well as from the effluents of sewage treatment works. To understand the presence of humics in water, a simplification of the elements interactions is shown in Fig. 1. Humics consist of numerous organic functions, particularly the carboxylic and phenolic groups, that have specific properties, such as the ability to ionise and to form complexes with metallic salts. Consequently, they can coagulate and be filtered through biofilters or membranes. However, they cover such a large molecular mass range (from one to several thousands daltons) that a satisfactory removal mechanism has been difficult to determine, prompting an investigation into this particular problem [1].

Equilibrium data from batch experiments provided valuable information regarding the adsorption of humic substances (HS) on granular activated carbon (GAC), iron coated activated alumina, AAFS, and ferric oxihydroxide in its beta form, akaganeite β-FeOOH [1]. However, water treatment works and industries usually operate on a continuous flow basis and the batch tanks are replaced by columns, filled with the adsorbent. Therefore, the need arose to reduce the size of the column down to a diameter still representative from the hydrodynamic aspect; too small a diameter, compared to the column length and the size of the adsorbent grains, might lead to a short circuit in the column [2–4]. The quality of the effluent treated through a column of GAC, AAFS or β-FeOOH will be determined and analytically modelled using both the Thomas and the Bed Depth Service Time models (BDST).

* Corresponding author. Tel.: +974 3166752; fax: +974 4852107/8.
E-mail address: m.khraisheh@qu.edu.qa (M. Khraisheh).

1385-8947/$ – see front matter © 2010 Elsevier B.V. All rights reserved.
doi:10.1016/j.cej.2010.04.043

Nomenclature

C_0	initial influent contaminant concentration (mg L^{-1})
C_t	effluent contaminant concentration at time t (mg L^{-1})
k_T	Thomas constant (L min^{-1} mg^{-1})
q_0	maximum adsorption capacity (mg g^{-1})
m	mass of adsorbent (g)
V	column throughput volume (L)
Q	flow rate (L min^{-1})
C_B	concentration of the effluent at time zero (mg L^{-1})
K_a	adsorption rate constant (L g^{-1} min^{-1})
N_0	column adsorption volumetric capacity (g L^{-1})
Z	bed depth (dm)
Q	flow rate (L min^{-1})
t_B	breakthrough time selected (the percentage of residual DOC in the effluent)
Z	bed depth
Z_c	critical bed depth, which corresponds to the Z value if t_B is equal to zero

The main aim of this column study is to predict how long the adsorbent will be able to sustain the removal of a specified amount of pollutant from solution before replacement or regeneration is needed (service time). The effect of molecular mass on the adsorption process is considered. The Thomas and BDST models are selected in this work and are used to predict and optimise the column operations. The Thomas and BDST models were applied to experimental data to predict the breakthrough curves and to determine the characteristic parameters of the column, a requirement for process design. Breakthrough curves are obtained from the column studies and are presented in this paper.

2. Materials and methods

2.1. Adsorbents and adsorbate

Granular activated carbon, GAC 207C, iron coated activated alumina (AAFS 50) and the ferric oxihydroxide in its beta form, β-FeOOH, were the adsorbents used in this study (characteristics of the adsorbents and suppliers are given in Table 1). Humic acid was obtained from (Aldrich, UK, lot number H1-675-2) in a powder form. This contains a broad range of molecular mass. Ultrafiltration was chosen to fractionate humic substances to produce solutions

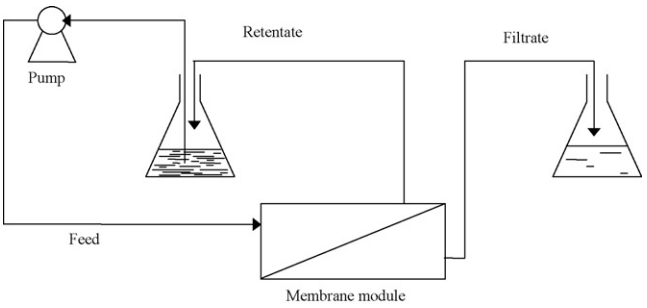

Fig. 2. Humic acid fractionation experimental set up.

with controlled molecular masses (MMs). The membranes used were polyethersulfone (PES) and Vivaflow 50 (from Sartorius Ltd., Epsom, Surrey, UK). Fig. 2 represents the experimental set up of the fractionation system used to separate the various fractions. The pump used for this separation process was a Watson Marlow (HR flow inducer, type MHRE 200). Solutions F1 (HS < 5 kDa), F12 (HS < 10 kDa) and F123 (HS < 50 kDa) were produced, stored in a dark fridge at 4 °C and were used within 3–4 weeks. Further details on the experiments can be found in [1]. The solution was diluted with deionised water to reach a dissolved organic content (DOC) of approximately 10 mg L^{-1}. The pH was adjusted to 7.0 using concentrated hydrochloric acid or sodium hydroxide as appropriate.

2.2. Continuous adsorption experiments

Each experiment was carried out in duplicate. Hydrodynamics in the column must be considered so as to avoid any short circuit, which would decrease the hydraulic residence time (HRT) of the humic substances solution (hence the contact time adsorbent–adsorbate) and would use the media unevenly. It is also of interest for bench experiments to reduce the size of the column so as to decrease both time and cost of experiments, especially given the difficulties involved in the separation of the various fractions of the humic substances. As a result, a 2.5 cm diameter was used to avoid potential wall effects (column diameter to grain median diameter ratio equals 54 [2–4]). The design parameters (flow rate, diameter, depth) satisfied criteria to avoid any wall effect. Sampling ports were made at 25 cm (port A), 40 cm (port B), 55 cm (port C) and 60 cm (port D) from the base of the column to correspond to an empty bed contact time (EBCT) of 19, 31, 43 and 47 min, respectively (Fig. 3). A diluted (1:50) F123 solution, HS MM < 50 kDa, with a neutral pH and a flow of 1.5 L/h was fed to the continuous system (Fig. 3).

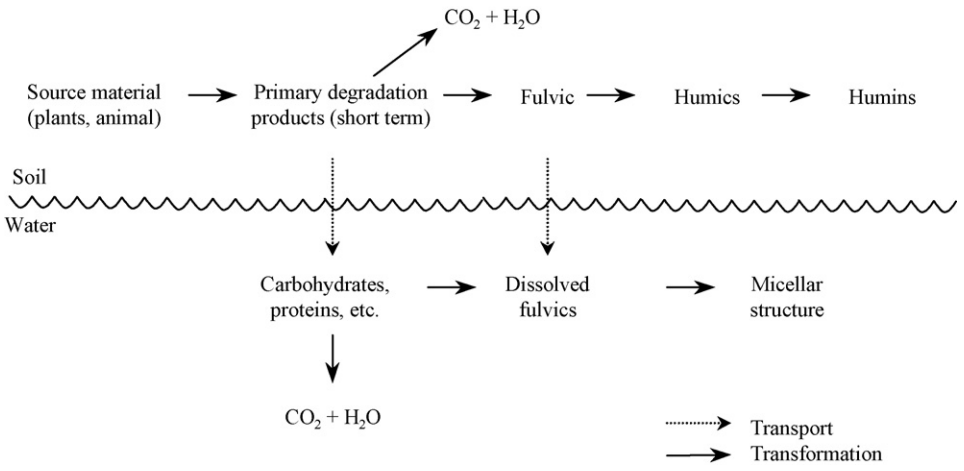

Fig. 1. The formation path way of humic substances.

Table 1
Adsorbent characteristics.

	GAC 207C	AAFS (50)	β-FeOOH
Supplier	Universal Mineral Supplies Ltd.	Alcan Chemicals	GEH Wasserchemie
Usual use	General purpose for liquid and vapour phase	New adsorbent	Drinking water for arsenic removal
Main component	High activity carbon	Amorphous, χ and γ forms of Al_2O_3, coated with iron sulfate	$Fe(OH)_3$ and β-FeOOH
Size of grains	Mesh 12–30 0.5–1.4 mm	Mesh 28–48 0.32–0.56 mm	0.32–2 mm
Surface area	1050 m^2/g	350–380 m^2/g	100 m^2/g

A 1 cm diameter microcolumn with bed depth of 10 cm, was used for the continuous adsorption test for HS solutions of low molecular masses. The use of smaller diameter columns reduced the need to maintain a large stock of solution for preparation and fractionation. Experiments and full analysis were performed of the compatibility of the results between the larger and the smaller diameter columns; full details are published elsewhere [5]. Sufficient volume of fraction F1 (<5 kDa) was fed into the microcolumn at 0.03 L/h, corresponding to an EBCT of 16 min.

Experiments were run as follows: (1) after washing to remove fine particles and particle size separation, adsorbent was poured into the column to make 60 or 10 cm of non-packed bed, respectively for the larger and smaller columns. This size was calculated to have an EBCT of between 10 and 45 min, and to be able to reach a 100% fluidisation; (2) a backwashing system was installed so as to feed the column from the effluent port (bottom of the column) with tap water. The adsorbent bed was fluidised to 100%, until no air or fines was left (water free of particles and bubbles). The longest time for this was the GAC, needing almost 12 h; (3) required amount and concentration of the humic solution was introduced to the system; (4) the backwashing system was disconnected and the normal down flow process started by switching the pumps on; (5) samples were taken from the ports and effluent (or effluent only for smaller columns) at designated times and (6) the effluent DOC (dissolved organic content) and UV spectra were then determined. A schematic of the process is depicted in Fig. 3.

2.3. DOC and SUVA analysis

Humic substances UV absorption spectra present a broad peak of absorbance centred on 254 nm. Therefore, UV absorbance at 254 nm (UV_{254}) is considered characteristic of these compounds. UV_{254} was measured on a double beam spectrophotometer (M350 double beam, Camspec Scientific Instruments Ltd., Sawston, Cambridge, UK). Dissolved Organic Carbon (DOC) analyses were performed on a Dohrman DC-80 Carbon Analyser, which uses the persulfate and UV oxidation, with an infrared carbon detector. Low molecular mass humics have a high DOC content but absorb little UV absorption. As a consequence, it may be observed that there is no decrease in UV absorbance after treatment, although low molecular masses may have been adsorbed. Conversely, a decrease in DOC does not indicate which type of humic substance has been adsorbed (high or low MM). Therefore, the third parameter of interest is the specific ultraviolet absorbance (SUVA) index, expressed as the ratio between the UV absorbance (in m^{-1}) and the DOC (in mg L^{-1}).

$$\text{SUVA} = \frac{UV_{254}}{DOC} \quad (1)$$

3. Results and discussion

3.1. Effect of column diameter

Hydrodynamics in the column must be considered so as to avoid any flow short circuits, which would decrease the hydraulic residence time (HRT) of the solution (hence the adsorbent–adsorbate contact time). It is also important to reduce the size of the column so as to decrease both time and cost of experiments, especially given the difficulties involved in the separation of the various fractions of the humic substances and the production of the low molecular mass fractions as discussed earlier. Microcolumns have been proved to give very good results in different contexts [2–4,6]. Li et al. [7] also suggest that the microcolumn technique could satisfactorily simulate the bed performance of large columns.

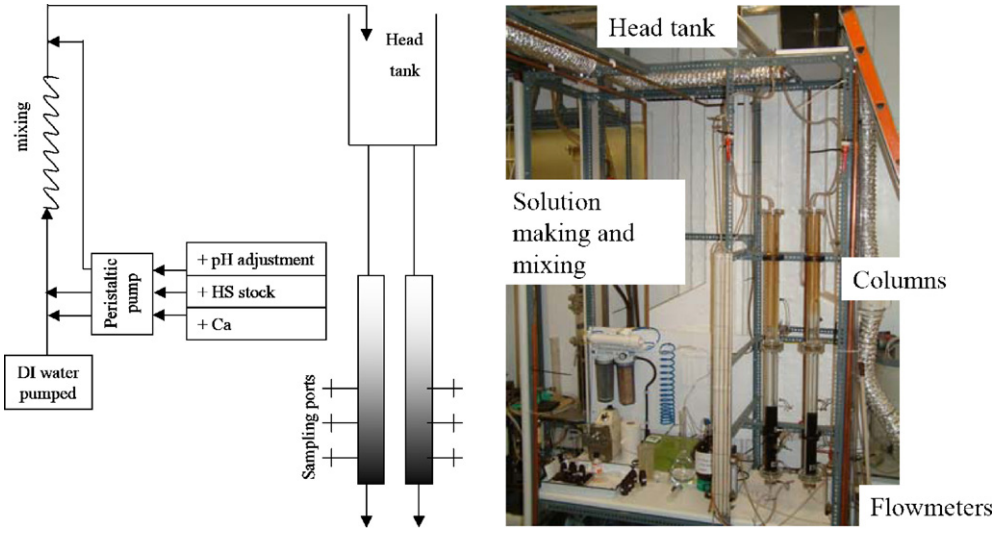

Fig. 3. Experimental set-up for column studies (showing columns 5 cm diameter).

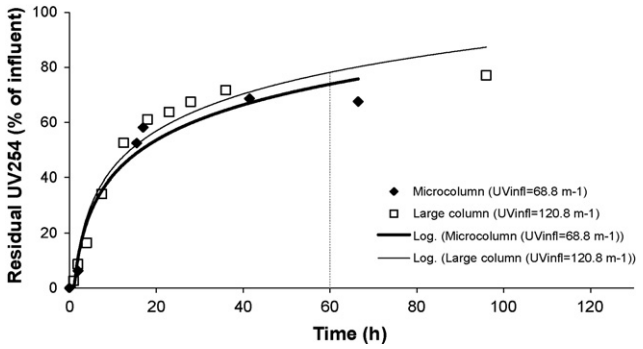

Fig. 4. Adsorption results of F123 solution compared on two different size columns (adsorbent was GAC, large column: 25 cm diameter, microcolumn: 1 cm diameter).

Columns of 2.5 cm diameter were initially used for adsorption of solution F123. The design parameters (flow rate, diameter and depth) satisfied the required criteria of avoiding any wall effect. For the microcolumn, the new diameter and bed depth were 1 and 10 cm, respectively. The flow rate was decreased to 38 cm/h compared to 76 cm/h for the larger columns. The new EBCT was 16 min.

From Fig. 4, it can be seen that the longer the run time, the more noticeable the differences were between the microcolumn and the large column. The large column gave slightly higher residual effluent UV absorbance. However, the difference between the results with the micro- and the large column were less than 5.6% after 60 h. Since most results are obtained with experimental times less than 60 h, for fraction F1, the difference was considered acceptable. For rigor, full statistical analyses were carried out; however, the results have not been presented in this paper. From these observations, it was concluded that the column studies could be carried out on the smaller column and would be comparable to the adsorption of F123 on the bigger columns [5].

3.2. Effect of humic substances molecular masses on the adsorption

3.2.1. Low molecular weigh HS (fraction F1 < 5 kDa)

The experiments for this fraction were carried out in the microcolumns. The DOC of influent F1 solution ranged between 6–7 mg L^{-1} and SUVA was 3–4. Figs. 5 and 6 show the percentage removal of UV_{254} and DOC, respectively. The breakthrough was observed on GAC after 90 h. Fig. 6 shows, over the range studied, the breakthrough was not recorded for the AAFS and β-FeOOH. During the first 5 h, residual UV absorbance and DOC were 15% remaining and 55% remaining, respectively on the GAC, and 30% remaining (UV) and 70% remaining (DOC) on AAFS and β-FeOOH.

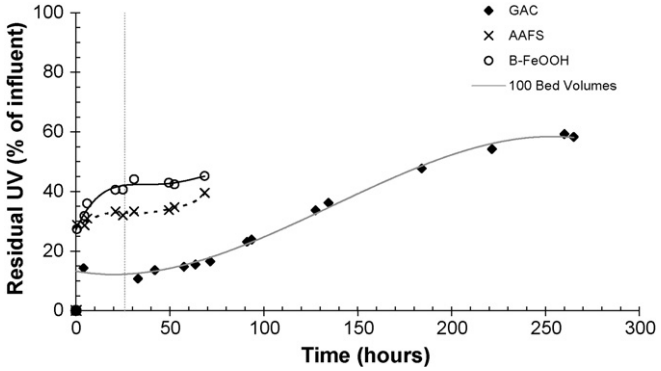

Fig. 5. Residual UV_{254} after adsorption of F1 on GAC, AAFS and β-FeOOH.

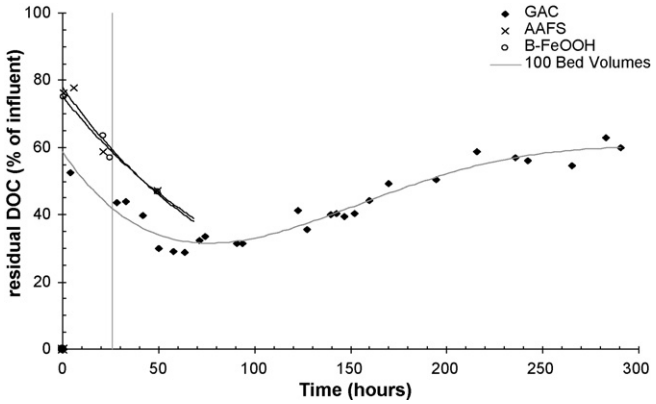

Fig. 6. Residual DOC after adsorption of F1 on GAC, AAFS and β-FeOOH.

The difference corresponds to retention of the heavy MM fractions in the column. After 5 h, the tendency is reversed and the residual UV absorbance started to increase as the residual DOC continues to decrease. After 20 h, a balance was achieved with a constant removal for the UV detectable organic matter (UV_{254}), while the DOC of the effluent continued to decrease and became constant (for the GAC system). Such behaviour indicates that the non-UV absorbing organic matter was removed. This was the case for the three adsorbent–adsorbate systems. A residual DOC effect was also observed by Teermann and Jekel [8] when reservoir water was treated (usually aquatic NOM are similar to F1 in terms of MM and SUVA) on a β-FeOOH adsorbent bed. An initial residual DOC of 10% remaining was immediately followed by a breakthrough. However, the residual of 80% remained stable for several weeks, which agreed closely with the present results on GAC, where the effluent DOC remains at 55% of the influent for at least 300 h (12.5 days). This may indicate that the diffusion occurring in the column is slow. This is also in agreement with results reported by Sontheimer and Hubele [9]. The effluent DOC was initially equal to the influent DOC (6.95 mg L^{-1}), i.e. 100% remaining before dropping to 90% remaining after a few days and down to 85% after 10 days.

Fig. 7 shows the evolution of the effluent SUVA with time, respectively when using GAC, AAFS and β-FeOOH. The SUVA of the effluent after being in contact with GAC is well below the SUVA of the influent. It shows that inside the column, the heavier MM of F1 was retained, and that the lightest MM was not adsorbed. Between 40 and 90 h, the DOC remained fairly constant while UV absorbance and SUVA start to increase, which indicates that the heavier MM of F1 exited the column. However, the stability of DOC implied that the lighter adsorbable MM of F1 (which does not absorb UV) was adsorbed indicating that no displacement between the lighter and heavier MM molecules took place. This is in contrast to what was observed by Gu et al. [20,21]. On the other hand, SUVA of the effluent increased after 5 h when using AAFS and β-FeOOH. It remained below the SUVA of the influent for AAFS, showing adsorption of the heaviest MM fractions of F1. Fettig [10] found that the EBCT on γ-Al_2O_3 was between 40 and 60 min for a breakthrough of 50% for removal of NOM at 200 bed volumes confirming the slow uptake nature of these adsorption processes.

3.2.2. Removal of fraction F12 (0–10 kDa)

The behaviour of F12 adsorption was found to be very different from fraction F1 (Fig. 8). On GAC, the breakthrough (after 5 h) had the typical S shape whereas on AAFS and β-FeOOH, the breakthrough was rather slow. The effluent DOC was high during the first 5 h for both iron compounds. Similarly to F1, a few hours were necessary before maximum DOC reduction. This is attributed, as before, to the necessity of accumulating HS in the solution (within the column) so as to reach a high enough concentration gradient,

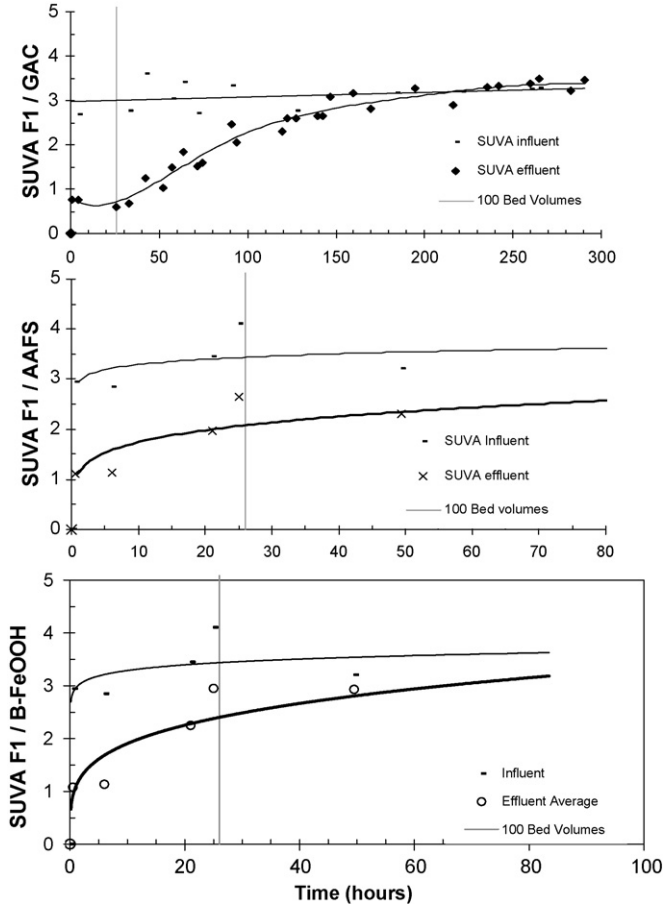

Fig. 7. Residual SUVA after adsorption of F1 on: (a) GAC; (b) AAFS; (c) β-FeOOH.

which will favor the diffusion to the adsorbent surface. Effluent DOC dropped to a minimum of 25%, of the influent value (i.e. approximately 2 mg L^{-1} for β-FeOOH), and 15% for UV_{254}, the breakthrough in this case occurred after 125 h.

The SUVA values showed which fraction is preferentially retained in the column. For F1, the minimum SUVA was approximately 1–1.5 in the effluent. This corresponded to the non-adsorbable HS portion of the solution. The constant removal of DOC (residual of 20% between 10 and 125 h) corresponds to a steady increase of the effluent's SUVA up to 4–5 indicating a gradual decrease in the adsorption of F1. After 125 h, the SUVA value slowly reaches the influent value, when F2 is not adsorbed more than F1.

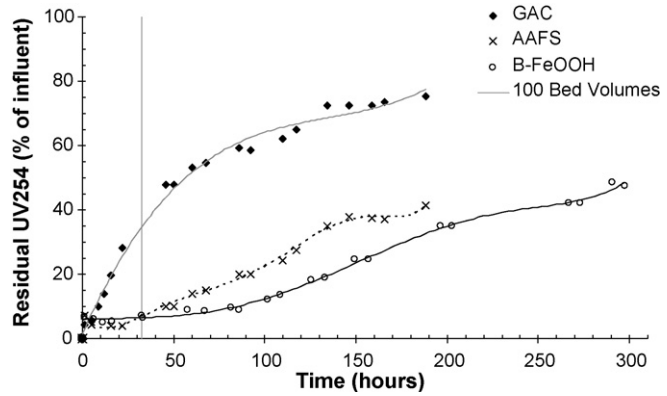

Fig. 8. Residual UV_{254} after adsorption of F12 on GAC, AAFS and β-FeOOH.

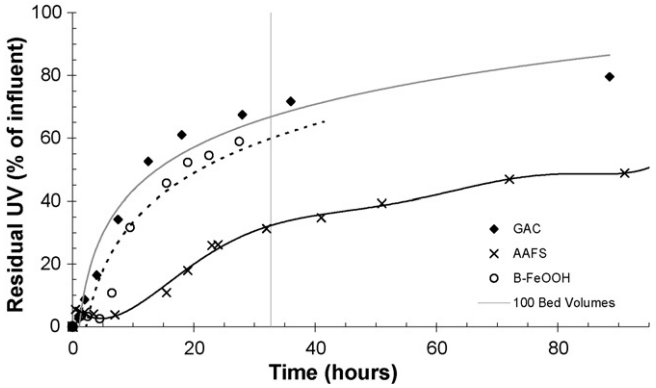

Fig. 9. Residual UV_{254} after adsorption of F123 on GAC, AAFS and β-FeOOH.

3.2.3. Removal of F123

The influent DOC was 12.5, 6.5 and 10 mg L^{-1} on GAC, AAFS and β-FeOOH media and the corresponding results are presented in Figs. 9 and 10 for UV absorbance and DOC of the effluent, respectively. It was observed that the breakthrough on GAC occurred very quickly, from UV absorbance results and after 3–4 h form DOC results. This confirms what was found from the equilibrium studies [1], i.e. that the heavier MM, mainly represented in F123 with up to 50 kDa, do not adsorb well on GAC due to the lack of external surface. This also strongly agrees with results obtained for the adsorption of pond water by GAC [11]. The authors observed that the breakthrough was slightly earlier for high MM natural organic matter and they attributed this behaviour to specific molecular interactions. As for the β-FeOOH, breakthrough occurs quickly too, immediately following the curve for GAC. However this is also attributed to a lower influent DOC. Overall, the iron oxihydroxide does not allow any removal of the lowest MM and AAFS is only slightly better. The intermediate MM were the best removed by adsorption on the iron compounds.

From Fig. 11, the initial decrease in DOC continued, but only on AAFS and β-FeOOH and not on GAC. Fig. 12 shows the SUVA of the effluent for adsorption of F123 on GAC, AAFS and β-FeOOH. On GAC, the SUVA of the effluent increased steeply, approaching the value of the influent SUVA indicating that no significant distinction is made in the distribution of the MM between the influent and the effluent. However, once the SUVA curve flattened, it remained constant and below the influent SUVA curve. It may be concluded that high MM humics are adsorbed on GAC to some extent. On the iron compounds, the increase is significant, although less steep on AAFS as expected from the slower breakthrough. The effluent's SUVA was also similar to the influent's SUVA.

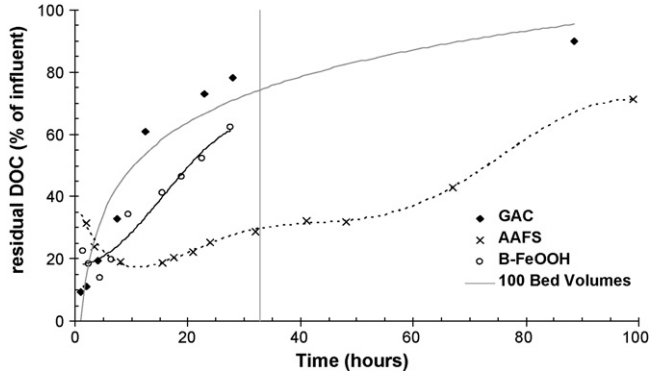

Fig. 10. Residual DOC after adsorption of F123 on GAC, AAFS and β-FeOOH.

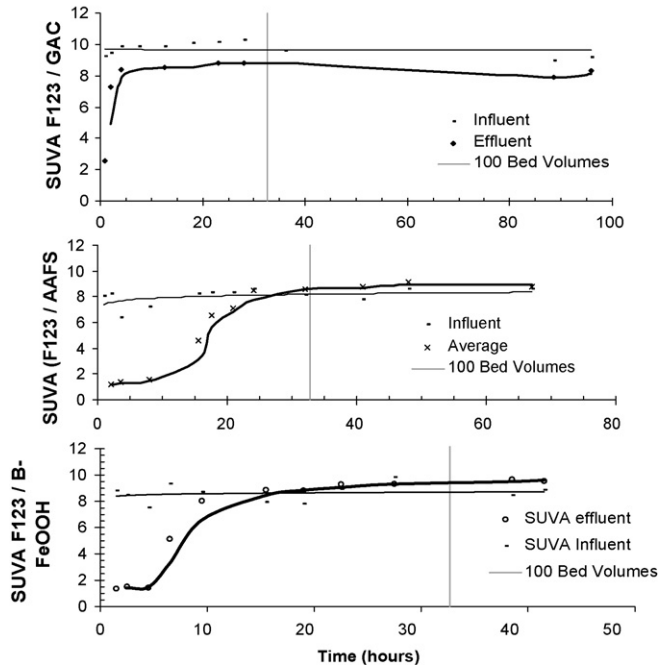

Fig. 11. Residual SUVA after adsorption of F123 on GAC, AAFS and β-FeOOH.

3.3. The Thomas model

The breakthrough curves were modelled using the Thomas model. This model is based on the ratio C_t/C_0 (effluent concentration at time t to influent concentration at time zero) versus the volume of solution treated and can be best described by Eqs. (2) and (3).

$$\frac{C_t}{C_0} = \frac{1}{1 + \exp[k_T(q_0 m - C_0 V)/Q]} \quad (2)$$

$$\ln\left(\frac{C_0}{C_t} - 1\right) = \left(\frac{k_T q_0 m}{Q}\right) - \left(\frac{k_T C_0}{Q}\right) V \quad (3)$$

where C_0 is the initial dye concentration (mg L^{-1}), C_t is the equilibrium concentration (mg L^{-1}) at time t (min), k_T is the Thomas constant (L min^{-1} mg^{-1}), Q is the volumetric flow rate (L min^{-1}), q_0 is the maximum column adsorption capacity (mg g^{-1}), m is the mass of adsorbent (g) and V is the throughput volume (L).

Hence, a plot of $\ln(C_0/C_t - 1)$ versus V gives a straight line with a slope of $(-k_T C_0/Q)$ and an intercept of $(k_T q_0 m/Q)$. Therefore, k_T and q_0 can be obtained.

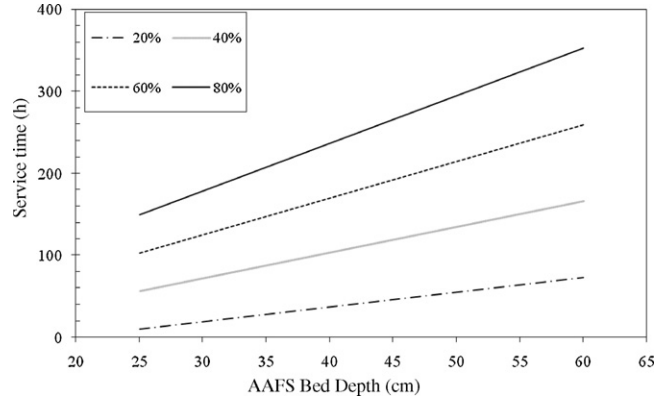

Fig. 12. The BDST model applied for adsorption of F123 on AAFS at different percentage breakthrough points ($100C_{eff}/C_{inf}$) (trend lines are presented since only two points were available on each adsorbent).

Table 2
Parameters[a] for the Thomas model and correlation coefficient.

	k_T (L h^{-1} mg^{-1})	q_0 (mg g^{-1})	R^2
F1/GAC	1.1×10^{-3}	9.59	0.9225
F12/β-FeOOH	1.0×10^{-3}	5.82	0.9323
F123/GAC	9.7×10^{-3}	1.64	0.8799
F123/AAFS	3.7×10^{-3}	2.02	0.9757
F123/β-FeOOH	6.5×10^{-3}	0.78	0.8910

[a] k_T is Thomas constant and q_0 is the maximum adsorption capacity.

The Thomas equation is one of the most general and widely used methods to predict the adsorption process [12]. The Thomas model, which assumes Langmuir kinetics of adsorption–desorption and no axial dispersion, is derived with the assumption that the rate driving force obeys second-order reversible reaction kinetics. Thomas' solution also assumes a constant separation factor but it is applicable to either favorable or unfavorable isotherms. The primary weakness of the Thomas solution is that its derivation is based on second-order reaction kinetics. Adsorption is usually not limited by chemical reaction kinetics but is often controlled by interphase mass transfer. This discrepancy can lead some error when this method is used to model adsorption process [12].

The estimated values of Thomas parameters are given in Table 2. The adsorption system results obtained from F1 on GAC were the only experimental data that fitted this model well for the whole range of data. For AAFS and β-FeOOH, the DOC decreased during the experimental period; therefore the model was not applicable for the earlier stages of the experimental runs, but fitted well for the data points corresponding to increasing DOC values. As expected, it was shown that GAC had a high capacity to absorb F1 (q_0). For F123, all results were lower with AAFS and is shown to be the best adsorbent for the highest MM represented in the working solution.

The parameter k_T corresponds to a rate constant and it is noticed that this is higher for F123 compared to values for F1 and F12 fractions. The increase, for higher MM humics, can be misleading since higher MM humic substances are thought to diffuse more slowly. However, it is suggested that the slow diffusion is compensated for by the accumulation of HS of higher MM close to the surface, which increases the concentration gradient, i.e. increases the driving force, and hence results in the higher diffusion rate.

3.4. Influence of bed depth and Bed Depth Service Time (BDST)

3.4.1. Influence of bed depth on F123 adsorption

Fig. 11a–c shows the residual DOC at different bed depths and different times for F123 adsorbed on GAC, AAFS and β-FeOOH, respectively. Here, the typical "S" shape that would indicate the presence of a mass transfer (MTZ), was not observed as the curves became wider indicating of a broader MTZ [13,14]. This can be attributed to a certain pore size (micropores smaller than 2.5 nm) not being accessible to the humic substances, which may be the case for heavier MM of F123. Only a small external surface area (less than 1 m^2/g) is left for adsorption of the heavy MM fractions on the carbon [15].

On GAC, residual DOC in the solution (tested for effluent withdrawn from the port A) reached 20% of the influent DOC. For effluent taken from port D (60 cm), the residual DOC decreased to 15% of the influent DOC only. It is concluded that the main mass transfer occurred in the first 25 cm and during the first 4 h of operation. On AAFS, the mass transfer took place in the top layers (25 cm), in three and a half hours (30% residual at 25 cm and at 60 cm). This strongly suggests that the MTZ is located in the first 25 cm and that the S shape would appear, should more samples were taken between 0 and 25 cm. β-FeOOH adsorption system behaved similarly, where the MTZ seems to be located in the first 10 cm of the

Table 3
Parameters[a] for the BDST model applied for adsorption of F123 on GAC, AAFS and β-FeOOH.

GAC	20%	40%	60%	80%
N_0 (mg L^{-1})	169.46	193.60	461.53	1891.63
N_0^* (mg g^{-1})	0.39	0.44	1.05	4.30
K_a (L mg^{-1} h^{-1})	<0	<0	0.0930	0.0034
Equation	$t_B = 0.18z + 0.23$	$t_B = 0.21z + 4.22$	$t_B = 0.49z - 0.86$	$t_B = 1.98z - 23.62$
Z_c (cm)	n.a.	n.a.	1.7	12
AAFS	20%	40%	60%	80%
N_0 (mg L^{-1})	930.90	1622.63	2314.57	3006.30
N_0^* (mg g^{-1})	1.05	1.82	2.60	3.38
K_a (L mg^{-1} h^{-1})	0.0043	0.0068	0.0169	<0
Equation	$t_B = 1.78z - 34.59$	$t_B = 3.13z - 21.66$	$t_B = 4.47z - 8.75$	$t_B = 5.80z + 4.18$
Z_c (cm)	19	7	2	n.a.
β-FeOOH	20%	40%	60%	80%
N_0 (mg L^{-1})	26.10	101.56	177.01	252.54
N_0^* (mg g^{-1})	0.02	0.08	0.13	0.19
K_a (L mg^{-1} h^{-1})	<0	<0	<0	<0
Equation	$t_B = 0.03z + 0.10$	$t_B = 0.14z + 7.08$	$t_B = 0.24z + 14.06$	$t_B = 0.34z + 21.04$
Z_c (cm)	n.a.	n.a.	n.a.	n.a.

[a] N_0^* (mg/g) calculated by multiplying N_0 by the bulk density of the adsorbent. Z_c is not calculable (n.a.) if $K_a < 0$.

column. The curve became almost vertical, respectively from 7.5 h on GAC, from 3.5 h on AAFS and from 2.5 h on β-FeOOH. The constant residual concentration, along the column depth, indicates that the depth does not have much influence on residual DOC. However, with time, the vertical curve continued to shift towards higher DOC in the effluent. As a consequence, it is concluded that the time factor is more important than the bed depth in these cases. This is actually in agreement with the kinetics which were shown to be slow and also with the fact that diffusion of heavy MM, which is the main constituents of solution F123, is very slow [5].

3.5. The Bed Depth Service Time (BDST) model

A different manner in which to approach the influence of the bed depth is to apply the Bed Depth Service Time model (BDST) represented in Eqs. (4)–(6), according to McKay and Bino [16] is the simplest method of predicting the column parameters.

$$\ln\left(\frac{C_0}{C_B} - 1\right) = \ln(e^{(K_a N_0 Z/Q)} - 1) - K_a C_0 t \quad (4)$$

The assumption on the exponential simplifies Eq. (4)

$$e^{(K_a N_0 Z/Q)} \gg 1 \Rightarrow \ln\left(\frac{C_0}{C_B} - 1\right) = \left(\frac{K_a N_0 Z}{Q}\right) - K_a C_0 t \quad (5)$$

From Eq. (5), the service time t at breakthrough is t_B and can be expressed using a linear equation:

$$t_B = \left(\frac{N_0}{C_0 Q}\right) Z - \frac{1}{K_a C_0} \ln\left(\frac{C_0}{C_B} - 1\right) \quad (6)$$

$$t_B = aZ + b \quad (7)$$

After identifying a and b for each group of constants, Eq. (6) becomes a simple relationship between the service time at breakthrough and the bed depth (Eq. (7)). A group of straight lines of t_B versus Z can be plotted, each line corresponding to a fixed value of C_0/C_B (i.e. a fixed percentage removal).

The results are shown in Table 3 and the parameters are calculated as described above. Values of N_0^* correspond to the BDST adsorption capacity and can be compared to q_0 calculated from the Thomas equation. The order of magnitude is similar and so is the classification for better adsorption capacity of F123 at 60% removal. However, GAC is shown to be the adsorbent with the highest capacity for 80% removal. This order is surprising when considering the large proportion of heavy MM in F123 and when compared with the adsorbents capacity calculated from the Freundlich model.

From Fig. 11, the breakthrough time to achieve a given DOC removal (%) at a given depth can be estimated. The selected percentage of removal of DOC was 20, 40, 60 and 80%. Selected depths correspond to the sampling ports, i.e. 25, 40, 55 and 60 cm (effluent) on GAC (the depth is expressed in dm when used in the equation). Only two ports were available for AAFS and β-FeOOH, but it is observed that the removal did not change greatly between the two ports during the first hours. On AAFS, the depths are 25 and 60 cm, for β-FeOOH, these are at 10 and 30 cm.

Plots of service time (corresponding to the estimated times described above) against the bed depth were obtained. This leads to a series of points for each chosen percentage of DOC removal. Using the BDST equation produces a straight line. Fig. 11 shows the plot for F123 adsorbed on AAFS. As mentioned above for AAFS and β-FeOOH, two points only were available for each selected percentage DOC removal. On GAC, this correlation was good with R^2 values between 0.94 and 0.99. Using GAC, there appears to be a noticeable benefit in increasing the bed depth if considering a breakthrough at 80% of the initial DOC. However, this particular line provokes doubts, especially when the calculation of the critical depth (in Table 2) is not consistent with other results. This is supported by Aksu and Gönen [12] who describe the slope of the BDST line as an indicator of the bed adsorbent capacity since the cross-section is kept constant in the column. Such a significant increase in the gradient of the slope cannot be due solely to an increased capacity when the three other slopes showed lower rate of increase. It is proposed that a different mechanism takes place. Such a mechanism might be a surface precipitation as has been suggested by Sperlich et al. [17]. The depth increase brings improvement on the service time for 60% breakthrough. For more stringent results (breakthrough at 20 and 40%), increasing the length beyond 25 cm does not bring a much higher service time as can be seen from the quasi-horizontal BDST line. The same phenomenon is observed for β-FeOOH where the service time is significantly increased if focusing only on a higher percentage breakthrough (lines are almost parallel but spaced wide apart). On AAFS, both bed depth and percentage breakthrough influence the service time. This agrees with previous results showing that AAFS was the best adsorbent for F123. It confirms that the very heavy MM were not retained on β-FeOOH and that F123 has little affinity for GAC. The explanation for this difference can be attributed to the mixing, which does not occur in the column. Since β-FeOOH does not present much internal porosity (it is mainly mesoporous), the external surface is used for adsorption. In the column and under water pressure, the bed compaction

increases, resulting in a decrease of the external surface. β-FeOOH poured porosity was 0.42 and decreased to 0.34 when packed. This is below the porosity of AAFS (0.50 and 0.47 for poured and packed) and of GAC (0.51 and 0.46).

When computed, K_a values in Table 2 do not show any obvious trend; this has been reported in previous studies [18]. However, K_a can still be compared with k_T in the Thomas equation (see Table 2). In general, it seems that K_a is larger than k_T (breakthrough 60–80%) hence BDST predicts a slightly faster transfer rate than the Thomas equation. Critical depth values follow opposite trends for GAC and AAFS. If the bed depth is equal to Z_c, or shallower, then the breakthrough will occur immediately (i.e. when $t_B = 0$). However it seems that Z_c is strongly dependent upon the adsorption capacity and transfer rate, hence the difficulty in interpreting these results. Finally, the bed depths reported in Table 3 confirms that the main Mass Transfer Zone occurred in the first 25 cm as suggested from Fig. 11. However, the bed depth of 12 cm to achieve 20% removal of DOC (breakthrough 80%) on GAC, is not consistent with the 1.7 cm necessary to remove 40% (breakthrough 60%), as discussed earlier. Critical bed depth to achieve 80% removal (20% breakthrough) and 60% removal (40% breakthrough) could not be computed due to a positive intercept of the BDST line. It appears that the short service time and the limited influence of the bed depth result in a positive intercept in the equation presented in Table 2, which in turn lead to a non-calculable critical bed depth.

Results on AAFS are consistent but no critical bed depth could be computed for β-FeOOH due to a positive intercept in the equation (Table 3). These results also show that the BDST model has its limitation. Particularly as it takes the N_0^* value as a constant whatever the bed depth considered. This is due to diffusion not being taken into account in the model [19].

4. Conclusions

The capacity of the adsorption column, of different sizes, for removing humic substances of a wide range of MM using GAC, AAFS or β-FeOOH, has been estimated. GAC was proved to adsorb humic substances well with MM below 5 kDa (F1), as expected from equilibrium studies. AAFS and β-FeOOH did not remove F1 to the same extent. For each adsorbent, a non-adsorbable fraction (low MM) was responsible for a residual DOC from the start of the run. It has also become clear that adsorption of heavier MM of each solution (F1, F12 and F123) requires a concentration gradient to build up in the column before any DOC removal in the effluent is observed; this was shown from the initial effluent DOC decrease. Prediction of the removal is also successful using the analytical method supplied by the Thomas equation. However this method is valid only from the time when the effluent DOC starts to increase. As for the BDST model (adsorption of F123), the Mass Transfer Zone is broad for each adsorbent. The contact time in the columns seems to be more important than the bed depth and most of the adsorption occurs in the top layers. The adsorbents are not completely exhausted when 80% breakthrough is reached. This gives further evidence of the slow diffusion of HS particularly for high MM.

References

[1] C.S. André, M. Khraisheh, Removal of humic substances from drinking water using GAC and iron-coated adsorbents: consideration of two kinetic models and the influence of mixing, Environmental Engineering Science 26 (1) (2009) 235–244.
[2] J. Fettig, H. Sontheimer, Kinetics of adsorption on activated carbon: I. Single-solute systems, Journal of Environmental Engineering 113 (4) (1987) 764–779.
[3] J. Fettig, H. Sontheimer, Kinetics of adsorption on activated carbon: II. Multisolute systems, Journal of Environmental Engineering 113 (4) (1987) 780–794.
[4] J. Fettig, H. Sontheimer, Kinetics of adsorption on activated carbon: III. Natural organic material, Journal of Environmental Engineering 113 (4) (1987) 795–810.
[5] S.C. Andre, Adsorption Treatment for the Removal of Humic Substances from Drinking Water Supply using Iron Coating Adsorbents, PhD thesis, University College London, London, UK, 2006.
[6] M. Al-Ghouti, M.A.M. Khraisheh, M. Ahmad, S.J. Allen, Microcolumn studies of dye adsorption onto manganese oxides modified diatomite, Journal of Hazardous Materials 146 (2007) 316–327.
[7] F. Li, A. Yuasa, K. Ebie, Y. Azuma, Microcolumn test and model analysis of activated carbon adsorption of dissolved organic matter after precoagulation: effects of pH and pore size distribution, Journal of Colloid and Interface Science 262 (2) (2003) 331–341.
[8] I.P. Teermann, M.R. Jekel, Adsorption of humic substances onto β-FeOOH and its chemical regeneration, Water Science and Technology 40 (1999) 199–206.
[9] H. Sontheimer, C. Hubele, The use of ozone and granular activated carbon in drinking water treatment, in: Treatment of Drinking Water for Organic Contaminants Proceedings of the Second National Conference on Drinking Water, Edmonton, Canada, April 7th and 8th, 1986, 1986.
[10] J. Fettig, Removal of humic substances by adsorption/ion exchange, Water Science and Technology 40 (9) (1999) 173–182.
[11] B. Schreiber, T. Brinkmann, V. Schmalz, E. Worch, Adsorption of dissolved organic matter onto activated carbon—the influence of temperature, absorption wavelength, and molecular size, Water Research 39 (2005) 3449–3456.
[12] Z. Aksu, F. Gönen, Biosorption of phenol by immobilized activated sludge in a continuous packed bed: prediction of breakthrough curves, Process Biochemistry 39 (2004) 599–613.
[13] M.Z. Othman, F.A. Roddick, R. Snow, Removal of dissolved organic compounds in fixed-bed columns: evaluation of low-rank coal adsorbents, Water Research 35 (12) (2001) 2943–2949.
[14] Y. Al-Degs, M. Khraisheh, S. Allen, Adsorption characteristics of reactive dyes in columns of activated carbon, Journal of Hazardous Materials 165 (2009) 944–949.
[15] A. Ersöz, R. Sa, A. Denizli, Ni(II) ion-imprinted solid-phase extraction and preconcentration in aqueous solutions by packed-bed columns, Analytica Chimica Acta 502 (2004) 91–97.
[16] G. McKay, M.J. Bino, Fixed bed adsorption for the removal of pollutants from water, Environmental Pollution 66 (1990) 33–53.
[17] A. Sperlich, A. Werner, A. Genz, G. Amy, E. Worch, M. Jekel, Breakthrough behaviour of granular ferric hydroxide (GFH) fixed-bed adsorption filters: modeling and experimental approaches, Water Research 39 (2005) 1190–1198.
[18] G.M. Walker, L.R. Weatherley, Adsorption of acid dyes on granular activated carbon in fixed beds, Water Research 31 (8) (1997) 2093–2101.
[19] D.C.K. Ko, J.F. Porter, G. McKay, Optimised correlation for the fixed bed sorption of metal ions on bone char, Chemical Engineering Science 55 (2000) 5819–5829.
[20] B. Gu, T.L. Mehlorn, L. Liang, J.F. McCarthy, Competitive adsorption, displacement, and transport of organic matter on iron oxide: II. Displacement and transport, Geochimica et Cosmochimica Acta 60 (1996) 2977–2992.
[21] B. Gu, T.L. Mehlorn, L. Liang, J.F. McCarthy, Competitive adsorption, displacement, and transport of organic matter on iron oxide: I. Competitive adsorption, Geochimica et Cosmochimica Acta 60 (1996) 1943–1950.